JOURNAL OF THEORETICAL AND APPLIED MECHANICS
51, 4, pp. 799-812, Warsaw 2013

AN ANALYSIS OF THE PRIMARY AND SUPERHARMONIC CONTACT RESONANCES – PART 3

Robert Kostek
University of Technology and Life Sciences in Bydgoszcz, Poland
e-mail: robertkostek@o2.pl

This paper presents a study of non-linear normal contact vibrations excited by an external harmonic force in a system containing two bodies being in planar contact. The system models, for instance, the slide unit of machine tools or positioning systems. The presented results, which are obtained both with numerical and perturbation methods, show clearly the evolution of resonance phenomena under various excitation amplitudes. Apart from the primary resonance, a number of super-harmonic resonances has been excited in the non-linear single-degree-of-freedom system. Hence, a resonance graph contains a number of peaks being below the natural frequency. The contact vibrations are associated with strongly non-linear phenomena like: asymmetry of vibrations, loss of contact, bending resonance peak, multi-stability, period-doubling bifurcations, chaotic vibrations, which are far from linear dynamics. These phenomena are presented and described in this article.

Key words: non-linear contact, vibrations, superharmonic resonance, multi-stability, bifurcation

1. Introduction

Dynamical contact problems play an important role in structural mechanics and machine tools vibrations to name but a few. Hence, certain models of contact are applied, for instance: finite element method (FEM), discrete element method (DEM) and multibody systems (MBS). The characteristic of the planar contact of rough surfaces is progressiveness, thus the contact is the most flexible under low contact pressure. Therefore, the contact deflection affect the behaviour of machines, which refers in particular to precision machines (Chlebus and Dybala, 1999; Fan *et al.*, 2012; Gutowski, 2003; Kaminskaya *et al.*, 1960; Levina and Reshetov, 1971; Marchelek, 1974; Shi and Polycarpou, 2005; Thomas, 1999). The contact deflections can be even larger than the distortion of machine parts (Chlebus and Dybala, 1999; Gutowski, 2003; Kaminskaya *et al.*, 1960; Levina and Reshetov, 1971; Marchelek, 1974). That leads to conclusions that certain parts of the machines can be modelled as rigid bodies, and contact characteristics significantly affect dynamical properties of the machines, for instance vibrations of machine tools (Gutowski, 2003; Marchelek, 1974). Chatter is a type of vibrations observed during machining, which makes machining unstable, less efficient and the machined surface rough (Dhupia *et al.*, 2007; Fan *et al.*, 2012; Gutowski, 2003; Huo *et al.*, 2010; Marchelek, 1974; Moradi *et al.*, 2010; Neugebauer *et al.*, 2007). Therefore, chatter can be reduced when excitation frequencies of the cutting force are far from the natural frequencies, while the natural frequencies of a machine tool depend on its contact interfaces.

Most of the articles deal with the primary contact resonance (Chajkin *et al.*, 1939; Grigorova and Tolstoi, 1966; Hess and Soom, 1991a,b; Kligerman, 2003; Rigaud and Perret-Liaudet, 2003; Tolstoi, 1967), while still a few describe the superharmonic contact resonances (Grudziński and Kostek, 2007; Kostek, 2004; Kostek, 2013a,b; Moradi *et al.*, 2010; Perret-Liaudet, 1998; Perret-Liaudet and Rigad, 2007); hence this paper presents a study of superharmonic contact

resonances. The superharmonic resonances appear below the natural frequency, which is an interesting phenomenon. And similarly to the primary resonance, they affect the dynamic properties of machine tools and chatter (Moradi *et al.*, 2010). These are the reasons why the evolutions of the superharmonic contact resonances due to various excitation amplitudes are investigated in this article. The vibrations are studied both with numerical and perturbation methods for various excitations, which provides valid information. Summarising, the contact vibrations have been found important in the context of the dynamics of precise machine tools, where low amplitudes of vibrations are required.

2. Theoretical fundamentals

The studied system has been formulated in the first part of this publication, thus certain information is repeated briefly (Kostek, 2013a). The system consisting of two bodies being in planar contact models a slide unit of a machine tool (Fig. 1a). The first body is a slider resting on the second body, whereas the second body is a massive fixed-base (slideway). The elastic nature of the bodies is neglected, thus they are assumed to be rigid bodies. The slider has one degree of freedom in the vertical direction, hence, normal displacement of the slider can be studied. The planar contact of rough surfaces (Fig. 1a) is modelled with a great number of microsprings and microdampers (Fig. 1b) which represent interacting roughness of asperities. After which, the homogenized contact (Fig. 1c) is modelled with one non-linear spring and damper (Figs. 1d,e). This leads to a non-linear single-degree-of-freedom system.

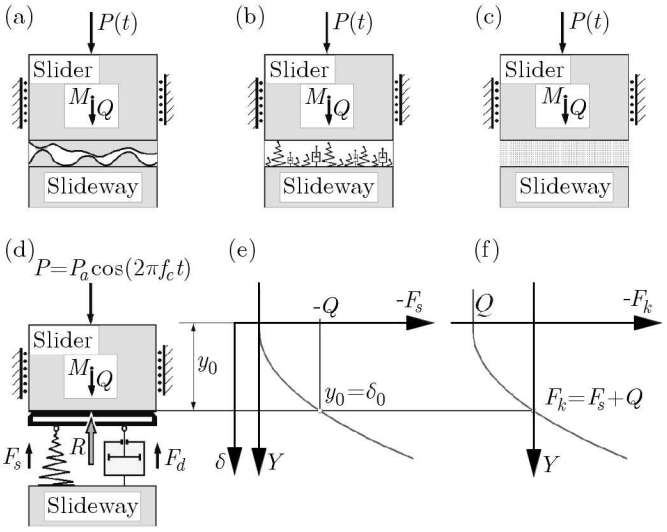

Fig. 1. Scheme of the considered dynamical system (a), and its physical models (b-d), characteristic of the spring force $F_s(e)$, characteristic of the conservative force $F_k(f)$

The displacement of the slider y is determined by the coordinate Y with respect to the rigid base (slideway). The co-ordinate system is pointing downwards (Fig. 1e) and its origin is fixed on the level where the contact deflection δ begins. Hence, the contact deflection equals the displacement when this displacement is positive, and the contact deflection equals zero when the displacement is below zero. That convention gives an opportunity to model the loss of contact – "gapping" – in the system. An important parameter is the static contact deflection due to weight of the slider, which determines the equilibrium position $\delta_0 = y_0$.

Three forces act on the slider, they are: the terrestrial gravity force, exciting (external, driving) harmonic force and the contact force. The terrestrial gravity force Q is defined as follows

$$Q = Mg \tag{2.1}$$

where Q denotes the terrestrial gravity force, M – mass of the slider $M = 0.2106\,\mathrm{kg}$, and g – acceleration of gravity $g = 9.81\,\mathrm{m/s^2}$, whilst the exciting harmonic force P is given by

$$P = P_a \cos(2\pi f_e t) \tag{2.2}$$

where P denotes the exciting harmonic force, P_a – amplitude of the exciting force, f_e – frequency of the excitation, and t – time. Then, the contact force (reaction) R can be treated as a sum of the spring force F_s and the damping force F_d (Fig. 1d), which are calculated from (Kostek, 2004; Martins *et al.*, 1990; Hunt and Crossley, 1975)

$$\begin{array}{llllll} \text{IF} & y > 0 & \text{THEN} & F_s = -Sc_n y^{m_2}, \quad \delta = y & \text{ELSE} & F_s = 0, \quad \delta = 0 \\ \text{IF} & y > 0 & \text{THEN} & F_d = -Sh_n y^l \dot{y} & \text{ELSE} & F_d = 0 \end{array} \tag{2.3}$$

where S denotes the nominal (apparent) contact area, δ is the normal contact deflection, while c_n, m_2, h_n, and l are parameters of the contact interface. The numerical values of the contact parameters have been identified from experimental results, and thus they are reliable; $S = 0.0009\,\mathrm{m^2}$, $c_n = 4.52E16\,\mathrm{N/m^4}$, $m_2 = 2$, $h_n = 3.5 \cdot 10^{11}\,\mathrm{Ns/m^4}$, $l = 1$ (Grudziński and Kostek, 2007; Kostek, 2002; Kostek, 2004). Lastly, the sum of the spring force F_s and the terrestrial gravity force Q can be treated as the conservative force

$$F_k = F_s + Q \tag{2.4}$$

The graph of the conservative force F_k is non-linear and asymmetrical (Fig. 1f), accordingly the studied contact vibrations are non-linear and asymmetrical as well. Finally, the investigated contact vibrations are described by the following non-linear differential equation

$$\ddot{y} = \frac{1}{M}[F_k(y) + Fd(y, \dot{y}) + P(t)] \tag{2.5}$$

The formulated differential equation of motion is non-linear because of the non-linearity of the spring and the damping contact forces, which predestines numerical and perturbation methods to solve this equation (Hess and Soom, 1991a,b; Kostek, 2013a,b,c; Nayak, 1972; Nayfeh, 1983; Nayfeh and Mook, 1995; Perret-Liaudet, 1998; Perret-Liaudet and Rigad, 2007).

The normal contact vibrations are linear when their amplitude is very small; then the natural frequency of the system equals $f_{n0} = 1485\,\mathrm{Hz}$ (Kostek, 2004). But when their amplitude becomes larger, then the vibrations become non-linear and certain characteristic phenomena appear (Grudziński and Kostek, 2007; Kostek, 2004; Kostek, 2013a). The vibrations become asymmetrical and multiharmonic; moreover, their resonance peak bends. At the same time, the amplitude of the m-th harmonic can be amplified significantly if its frequency is near the natural frequency, which in turn introduces superharmonic resonances. The resonance frequencies are given by

$$f_e \approx \frac{1}{m} f_{n0} \tag{2.6}$$

where f_e denotes the excitation frequency of the $1/m$ superharmonic resonance, f_{n0} – natural frequency, while m is a positive integer. Thus, the resonance peaks are observed below the natural frequency. More information about non-linear resonances is presented in literature (Awrejcewicz, 1996; Belhaq and Fahsi, 2009; Bogusz *et al.*, 1974; Cunningham, 1958; Fyrillas and Szeri, 1998; Grudziński and Kostek, 2007; Kostek, 2004; Kostek, 2013a; Nayfeh and Mook, 1995; Parlitz and Lauterborn, 1985; Tang, 2000; Thompson and Stewart, 2002).

3. Analysis of contact resonances

First, an increase of the excitation amplitude from $P_a = 0.50Q$ to $P_a = 0.60Q$ makes the amplitudes of the main resonance and the 1/2 superharmonic resonance growing; thus in turn the bistability and multistability areas become larger (Figs. 2a,b, 3a,b). The phenomenon of multistability has been presented previously (Kostek, 2013a). At the same time, the amplitudes of the 1/3 and 1/4 superharmonic resonances become larger, thus, in turn, the resonances are visible in Figs. 2a,b, 3a,b.

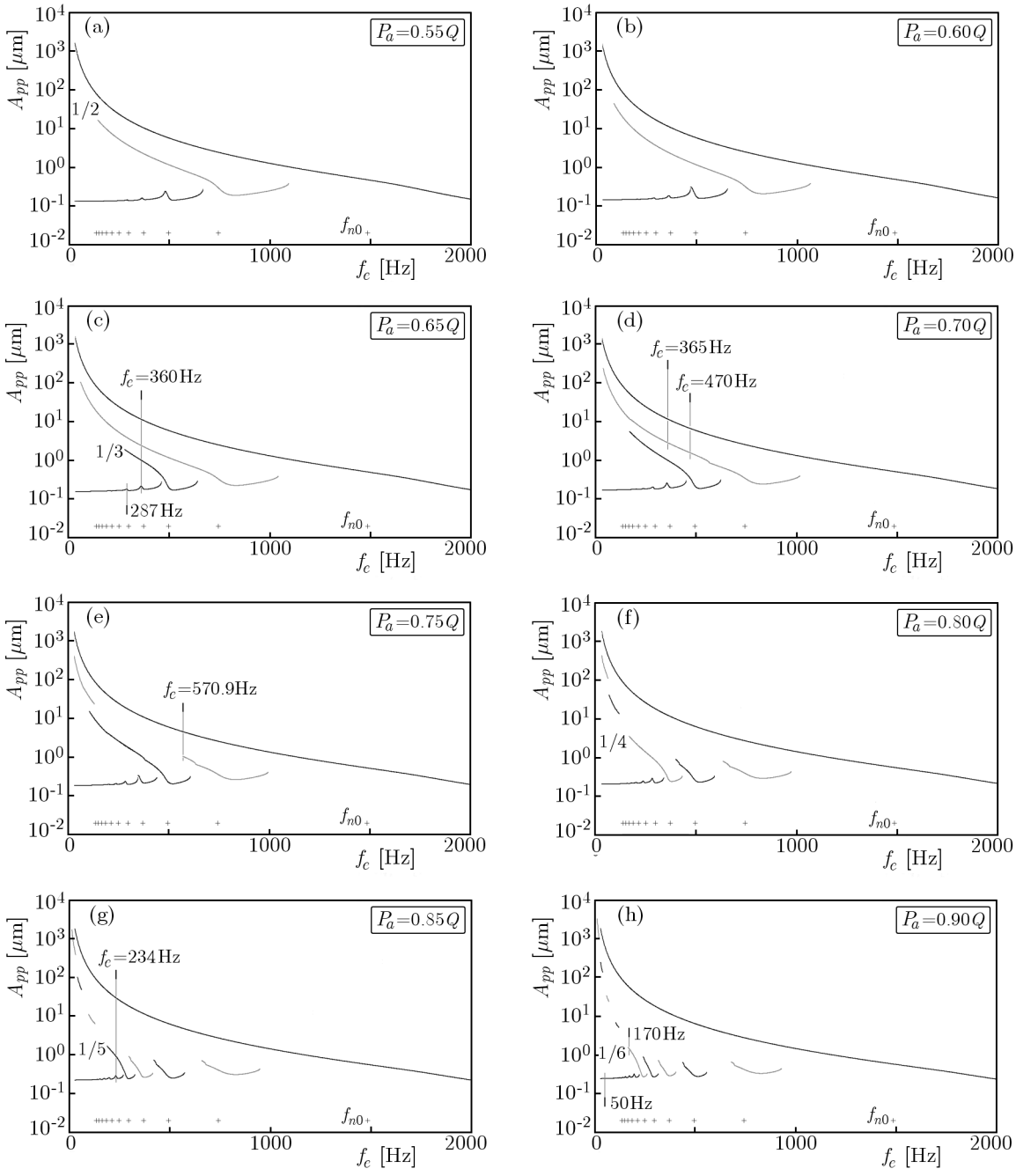

Fig. 2. Graphs of the contact resonances; peak-to-peak amplitude $A_{pp} = y_{max} - y_{min}$ against the frequency of excitation f_e; plus signs (+) represent resonant frequencies $f_e \approx f_{n0}/m$, Eq. (2.6)

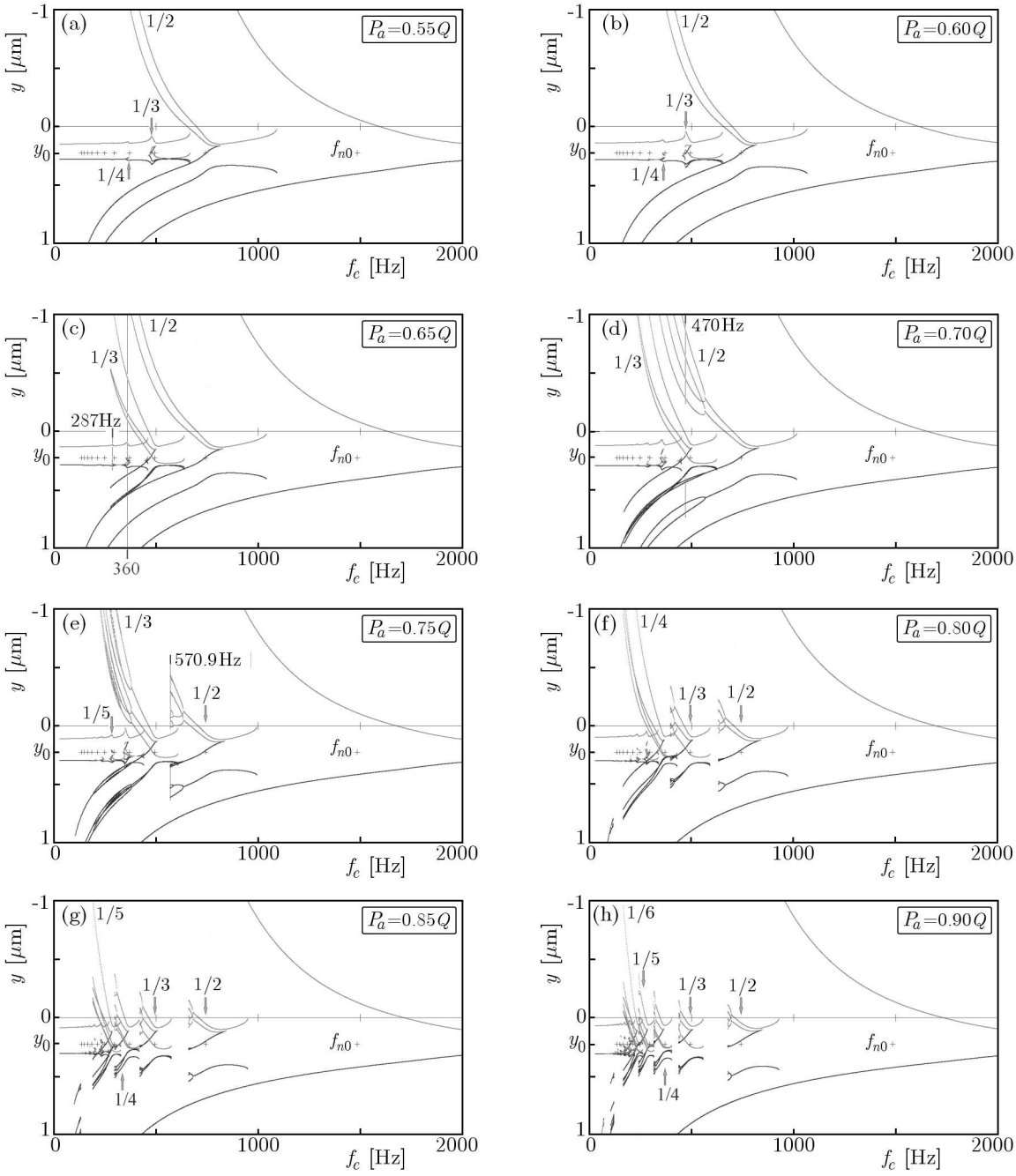

Fig. 3. Graphs of the contact resonances; local extrema of time histories against the frequency of excitation f_e; (gray line – minima, black line – maxima, obtained with the numerical method)

Then, the further increase of the excitation amplitude up to $P_a = 0.65Q$ leads to bending of the 1/3 superharmonic resonance peak; therefore, four resonances can be excited at a certain excitation frequency, see Figs. 2c, 3c. They are:

1. main resonance,
2. 1/2 superharmonic resonance,
3. 1/3 superharmonic resonance and
4. 1/4 or 1/5 superharmonic resonance.

The vibrations excited at frequencies $f_e = 360\,\text{Hz}$ and $f_e = 287\,\text{Hz}$ are presented in the next Section (Figs. 4, 5). It should be mentioned that 1/4 and 1/5 superharmonic resonances cannot be excited at the same frequency, because the 1/4 superharmonic resonance peak does not bend for $P_a = 0.65Q$ (Figs. 2c, 3c).

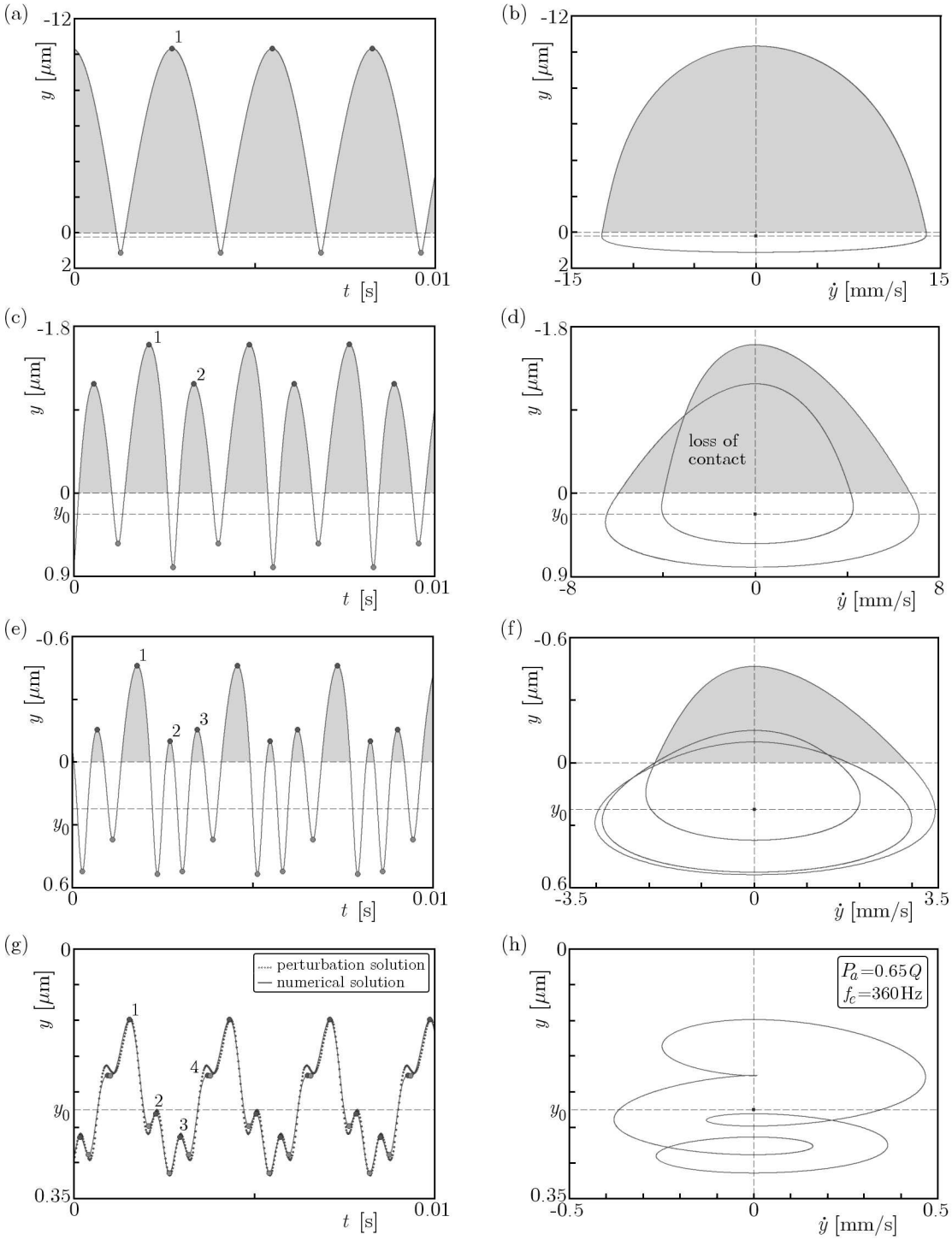

Fig. 4. Time histories of the displacement (a, c, e, g), and phase portraits of vibrations (b, d, f, h), of the primary resonance (a, b), 1/2 superharmonic resonance (c, d), 1/3 superharmonic resonance (e, f), and 1/4 superharmonic resonance (g, h), excited by a harmonic force of $P_a = 0.65Q$, $f_e = 360\,\text{Hz}$. A number of local minima is observed over one cycle of the excitation: one (a), two (c), three (e), and four (g)

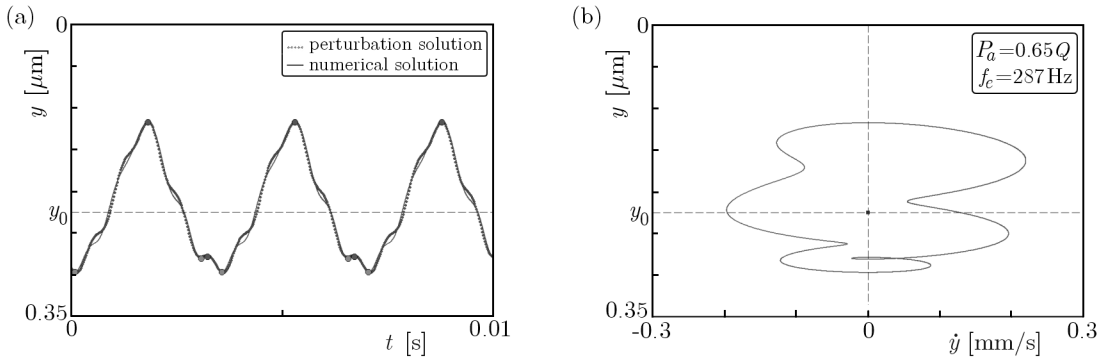

Fig. 5. Time history of the displacement (a), and phase portrait (b), of the 1/5 superharmonic resonance vibrations excited by a harmonic force of $P_a = 0.65Q$, $f_e = 287\,\mathrm{Hz}$

Next, for the excitation amplitude being $P_a = 0.70Q$, opposing period-doubling bifurcations at the 1/2 superharmonic resonance appear. Thus, incomplete period-doubling cascade (Thompson and Stewart, 2002) can be observed. One of these bifurcations is visible in Fig. 3d. Between these two opposing period-doubling bifurcations, eight curves forming closed loops represent the resonance in Fig. 3d. The number of the curves is associated with the number of extrema observed during one period of vibrations. The extrema are presented in the time history of displacement in Fig. 6a. More information about the evolution of the 1/2 superharmonic resonance will be presented in a new article.

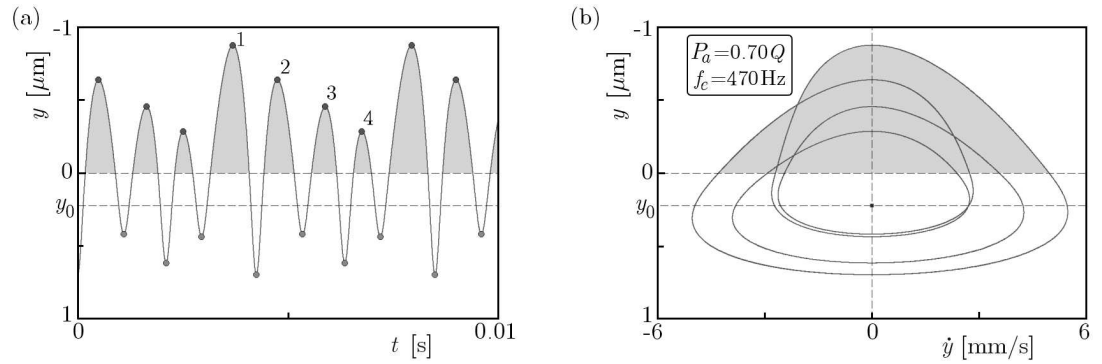

Fig. 6. Time history of the displacement (a), and phase portrait (b), of the 1/2 superharmonic resonance vibrations after first period-doubling bifurcation excited by a harmonic force of $P_a = 0.70Q$, $f_e = 470\,\mathrm{Hz}$. Four local minima are observed over two cycles of the excitation

After that, for an excitation amplitude being $P_a = 0.75Q$, the branch of the 1/2 superharmonic resonance is divided into two parts (Figs. 2e, 3e) by two opposing cascades of bifurcations leading to chaos. Therefore, the solution being near 100 Hz is isolated from other attractors and a gap between these two parts of the 1/2 superharmonic resonance appears. Hence, the isolated part cannot be found with a sweeping signal; accordingly, a special procedure must be applied to find one. Moreover, an incomplete period-doubling cascade is observed at the 1/3 superharmonic resonance; thus a number of curves represent the resonance in Fig. 3e. At the same time, amplitudes of the 1/4 and 1/5 superharmonic resonances become larger, thus the resonances are visible in Figs. 2e, 3e.

Some interesting phenomena are observed, when the excitation amplitude equals $P_a = 0.80Q$. Likewise, as previously, the branch of the 1/2 superharmonic resonance is divided into two parts, but the gap is larger (Fig. 2f). Thus, in consequence, the part of the 1/2 superharmonic resonance being near half of the natural frequency ($f_e = 800\,\mathrm{Hz}$) is isolated from the 1/3 superharmonic resonance. Similarly, the part of the 1/2 superharmonic resonance being near $f_e = 50\,\mathrm{Hz}$ is

isolated from other attractors. Likewise, the 1/3 superharmonic resonance is divided into two parts, by two opposing cascades of bifurcations leading to chaos (Figs. 2f, 3f). The chaotic vibrations of the 1/3 superharmonic resonance have been previously studied (Grudziński and Kostek, 2007; Kostek, 2004). Furthermore, the peak of the 1/4 superharmonic resonance bends, which is a result of an increase of the excitation amplitude and the amplitude of the resonance.

Next, an increase of the excitation amplitude up to $P_a = 0.85Q$ makes the gap of the 1/2 superharmonic resonance larger; hence the two parts of the resonance get smaller (Figs. 2g, 3g). A similar phenomenon is observed for the 1/3 superharmonic resonance too. Meanwhile, the aforementioned 1/4 superharmonic resonance is divided into two parts by two opposing cascades of bifurcations. Moreover, the peak of the 1/5 superharmonic resonance bends due to the increase of the excitation amplitude. Therefore, three resonances can be excited at frequency $f_e = 234\,\mathrm{Hz}$ (Figs. 2g, 3g, 7). They are:

1. main resonance,
2. 1/5 superharmonic resonance and
3. 1/6 superharmonic resonance.

That is the phenomenon of multistability.

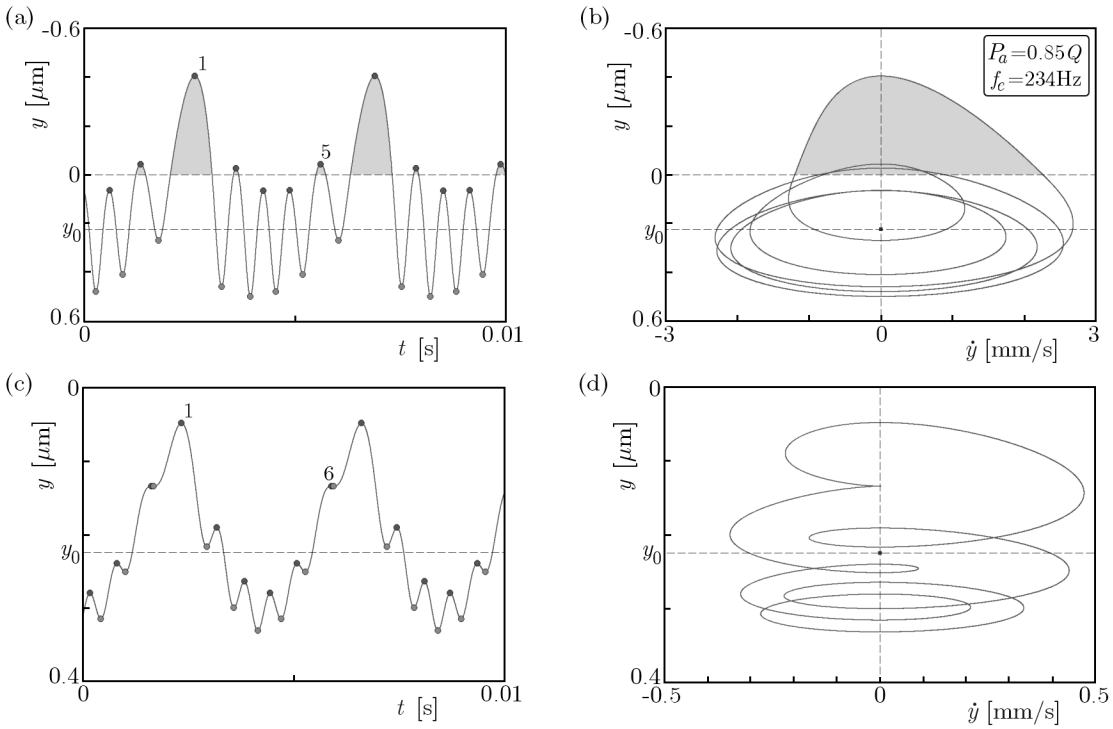

Fig. 7. Time histories of the displacement (a, c), and phase portraits of vibrations (b, d), of the 1/5 superharmonic resonance (a, b), and 1/6 superharmonic resonance (c, d), excited by a harmonic force of $P_a = 0.85Q$, $f_e = 234\,\mathrm{Hz}$. A number of local minima is observed over one cycle of the excitation: five (a), and six (c)

Last, due to an increase of the excitation amplitude up to $P_a = 0.90Q$ the gaps of the 1/2, 1/3 and 1/4 superharmonic resonances become larger. Therefore, small isolated parts of the 1/2 and 1/3 superharmonic resonances being near $f_e = 800\,\mathrm{Hz}$ and $f_e = 500\,\mathrm{Hz}$ are visible in Figs. 2h, 3h, while the 1/5 superharmonic resonance peak is divided into two parts by two opposing cascades of period-doubling bifurcations. At the same time, the amplitude of the 1/6 superharmonic resonance is growing (Figs. 7c, 8a), thus in turn its resonance peak bends (Figs. 2h, 3h). Also vibrations being below the resonant frequencies during an increase of the excitation force amplitude become gradually more non-linear and more asymmetrical, see Fig. 9.

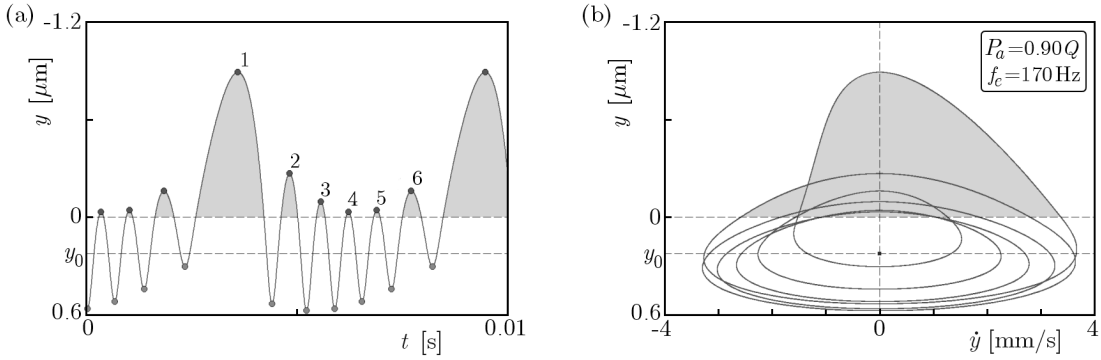

Fig. 8. Time history of the displacement (a), and phase portrait of vibrations (b), of the 1/6 superharmonic resonance excited by a harmonic force of $P_a = 0.90Q$, $f_e = 170\,\mathrm{Hz}$. Six local minima are observed over one cycle of the excitation

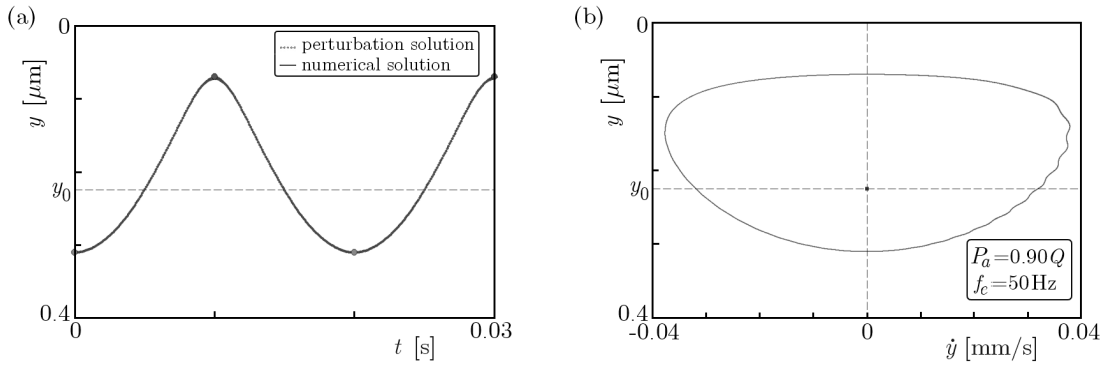

Fig. 9. Time history of the displacement (a), and phase portrait of vibrations (b), being below resonances (quasistatic process) excited by a harmonic force of $P_a = 0.90Q$, $f_e = 50\,\mathrm{Hz}$

The presented results clearly show the evolution of the superharmonic resonances. First, their amplitudes are growing with an increase of the excitation amplitude; next their peaks bend; and then incomplete period-doubling cascades appear. After that, the period-doubling cascades lead to chaotic motion. And finally, the period-doubling cascades divide a superharmonic resonance into two separate parts. With a further increase of the excitation amplitude, the two parts become smaller and the gap becomes lager. The phenomena are observed gradually with an increase of the excitation amplitude, first for the 1/2 superharmonic resonance, and then for the 1/3, 1/4, 1/5, and finally, the 1/6 superharmonic resonances. The higher harmonics need a larger excitation amplitude to become significant. Moreover, the evolution of the superharmonic resonances becomes faster with an increase of the excitation amplitude. That in short presents the evolution of the superharmonic resonances. The main resonance has been simulated at frequencies of excitation being from $f_e = 30\,\mathrm{Hz}$ to $f_e = 2000\,\mathrm{Hz}$. The visualization of the contact resonances is available on the internet https://www.youtube.com/watch?v=cNRU-TUXCao.

4. Analysis of contact vibrations

In this Section, contact vibrations excited for various magnitudes of the excitation frequency and the excitation amplitude are studied. The obtained time histories of displacement and phase portraits of contact vibrations are presented in Figs. 4-9. Although the vibrations are various, they have some common features, which are described below. The vibrations are asymmetrical with respect to the equilibrium position y_0, because different values of the conservative force are obtained for the same displacement magnitude, depending on whether the displacement is up or

down from the equilibrium position (Fig. 1f). Therefore, phase portraits have an asymmetrical shape. The asymmetry of the contact vibrations is visible in Fig. 3 too. The contact vibrations are not harmonical, they have a multi-harmonic nature because both the conservative and damping force are non-linear. Accordingly, the phase portraits have a non-elliptical shape.

First, the main resonance and the 1/2, 1/3, and 1/4 superharmonic resonances, excited by the external force of the frequency $f_e = 360\,\mathrm{Hz}$ and amplitude $P_a = 0.65Q$ are studied (Figs. 2c, 3c, 4). This external force can excite four resonances, which is the so-called multi-stability.

The contact micro-vibrations of the main resonance are the most asymmetrical because their amplitude is the largest, see Fig. 4a. Hence, their phase portrait has a non-elliptical shape (Fig. 4b). Moreover, the slider periodically loses contact with the slideway, and the minima reach negative values (Figs. 4a,b). One minimum is observed during one period of vibrations, and the orbit point circumnavigates the origin once during one period. Consequently, two curves represent the main resonance in Fig. 3c. At the same time, for the 1/2 superharmonic resonance, two minima and two maxima are visible during one period in Fig. 4c. Hence, the orbit point circumnavigates the origin twice (Fig. 4d). Accordingly, four curves represent the resonance in Fig. 3c. The amplitude of these vibrations is large, thus the loss of contact is visible in Figs. 4c,d.

The amplitude of the 1/3 superharmonic resonance is smaller compared with the aforementioned resonances, but still the vibrations are very asymmetrical and the loss of contact is visible (Fig. 4e). Three minima and three maxima are observed over one period in Fig. 4e, and thrice the orbit point circumnavigates the origin (Fig. 4f). Hence, six curves represent the resonance in Fig. 3c. It should be mentioned that the phase portrait has a complex shape.

Although the amplitude of the 1/4 superharmonic resonance is small (Fig. 3c), its vibrations are sophisticated. Four minima and four maxima are observed over one period of vibrations (Fig. 4g); hence eight curves represent this resonance in Fig. 3c. Moreover, some loops are visible in the phase portrait, thus one has a complex shape (Fig. 4h). The vibrations are studied both with perturbation and numerical methods. The obtained results show good agreement (Fig. 4g), which leads to the conclusion that the previously presented perturbation solution well describes this resonance (Kostek, 2013a,b).

The 1/5 superharmonic resonance excited by the external force of the frequency $f_e = 287\,\mathrm{Hz}$ and amplitude $P_a = 0.65Q$ is studied both with the perturbation and numerical methods. The obtained results show good agreement (Fig. 5a), hence the perturbation solution well reflects the nature of this resonance. In spite of the fact that the amplitude of the 1/5 superharmonic resonance is small, its vibrations are sophisticated. The vibrations are asymmetrical and multi-harmonic. Moreover, the phase portrait has a complex shape (Fig. 5b). This resonance is at an early stage, thus only two minima and two maxima are observed over one period of vibrations. Hence four curves represent this resonance in Fig. 3c.

The vibrations of the 1/2 superharmonic resonance excited by the external force of the frequency $f_e = 470\,\mathrm{Hz}$ and amplitude $P_a = 0.70Q$ are presented in Fig. 6. In this case, the period of these vibrations is doubled due to the period-doubling bifurcation (Fig. 3d). Thus four minima and four maxima are visible over two periods of excitation (Fig. 6a), hence eight curves represent the resonance in Fig. 3d. Accordingly, the orbit point circumnavigates the origin four times (Fig. 6b). The amplitude of these vibrations is large, thus the loss of contact is visible in Figs. 3d and 6. These vibrations (Fig. 6) can be compared with the vibrations presented before, in Figs. 4c,d. Summarising this, the period-doubling bifurcation makes the vibrations more sophisticated, more extrema appear over one period of vibrations, the period of vibrations is doubled, the phase portrait has a more complex shape, and a subharmonic frequency appears $(f_e/2)$.

Three resonances can be excited by the external force of the frequency $f_e = 234\,\mathrm{Hz}$ and amplitude $P_a = 0.85Q$ (Fig. 2g). But only two are presented in Fig. 7, and they are the 1/5 and 1/6 superharmonic resonances. First, for the 1/5 superharmonic resonance, five minima and

five maxima are visible over one period of excitation (Fig. 7a), thus ten curves represent the resonance in Fig. 3g. Accordingly, the orbit point circumnavigates the equilibrium position five times (Fig. 7b). The amplitude of these vibrations is large, thus the loss of contact is visible in Figs. 3g and 7a,b. In this case, the perturbation solution does not hold because of the loss of contact. The vibrations of the 1/5 superharmonic resonance being at the early stage are presented in Fig. 5, which clearly shows the evolution of the 1/5 superharmonic resonance due to an increase of the excitation amplitude. Finally, the 1/6 superharmonic resonance is presented in Figs. 3g, 7cd. These vibrations are asymmetrical and multi-harmonic. Moreover, a number of loops are visible in Fig. 7d, thus the phase portrait has a complex shape. In this case, the resonance is at an early stage, but six minima and six maxima are observed over one period of vibrations in Fig. 7c. Hence, twelve curves represent this resonance in Fig. 3g.

An increase of the excitation amplitude up to $P_a = 0.90Q$ makes the amplitude of the 1/6 superharmonic resonance grow, thus, with the frequency of excitation $f_e = 170\,\mathrm{Hz}$ a loss of contact is visible in Figs. 3h and 8. Moreover, on a phase portrait, the orbit point circumnavigates the equilibrium position six times, over one period of vibrations (Fig. 8b).

The vibrations that are below the resonant frequencies are visible in Fig. 9. This shows quasistatic vibrations, which are non-linear, asymmetrical and multi-harmonic. The time history of displacement and the phase portrait have characteristic shapes which are different from others presented in this article. These vibrations are studied both with the perturbation and numerical methods. The obtained results show excellent agreement (Fig. 9a), which leads to the conclusion that the perturbation solution describes these vibrations well. The vibrations take place when the contact interface is loaded by a low frequency external force, which is very common in industrial practice. Hence, the vibrations have been studied previously by researchers (Kostek, 2004; Skrodzewicz, 2003; Skrodzewicz and Gutowski, 2000). It should be mentioned that the presented perturbation solution has a similar structure to the model presented by Skrodzewicz (2003), in spite of the fact that the author shows a different approach to the phenomenon.

Summarising this, the contact vibrations (Figs. 4-9) are strongly non-linear; therefore, some characteristic phenomena are observed. The vibrations are sensitive to the magnitude of the excitation frequency and the excitation amplitude; hence a small change of the parameters can significantly change the obtained results. Moreover, the vibrations are sensitive to initial conditions too, which is a result of the multistability; because a number of solutions can be obtained for identical excitations. Finally, a number of minima are observed over one period of vibrations. The number depends on the parameters of excitation and the kind of excited vibrations. The number corresponds with the integer m, which indicates a superharmonic resonance (Eq. 7). This phenomenon reflects the multi-harmonic nature of contact vibrations. In conclusion, the vibrations are far from the dynamics of a linear single-degree-of-freedom system.

5. Conclusions

This article presents the evolution of non-linear normal contact vibrations and contact resonances, which are important in the context of precision machining and machine tools vibrations. These vibrations have been studied both with numerical and perturbation methods. The obtained results show good agreement, which leads to the conclusion that the perturbation solution describes the contact vibrations well. The vibrations have been studied for a wide range of excitations, which provides valid information.

The contact vibrations are non-linear, which leads to asymmetry of vibrations, "gapping", superharmonic resonances, multi-stability, complex motion and chaotic motion (Grudziński and Kostek, 2007; Kostek, 2004). The kinematics of contact vibrations is complex, which is a result of the multiharmonic nature of these vibrations and magnification of higher harmonics. The

magnification of the higher harmonics is associated with the superharmonic resonances. Accordingly, a number of minima are observed over one period of vibrations. This number, which depends on the excitation parameters, kinds of vibrations, and the kind of the excited resonance, corresponds to m, see Eq. (2.6). In consequence, these phenomena make the shape of the phase portraits complex.

Moreover, the evolution of the superharmonic resonances has been studied. At the beginning, the amplitude of a superharmonic resonance is growing with an increase of the excitation amplitude. Then, its peak bends, which introduces multistability. Next, an incomplete period-doubling cascade appears. After that, it changes into two opposing period-doubling cascades leading to chaos. At last, a branch of the superharmonic resonance is divided into two separate parts. Finally, the separate parts of the resonance become smaller with an increase of the excitation amplitude. At the same time, the gap between these two separate parts becomes larger. The following stages of the evolution are observed first, for the 1/2 superharmonic resonance, and then for the 1/3, 1/4, 1/5 and 1/6 superharmonic resonances. The amplitudes of these resonances become smaller, and their vibrations become more complex, with an increase of the integer m, while the evolution of these resonances becomes faster with an increase of the excitation amplitude.

This summarises the evolution of the contact resonances and shows the complex nature of the normal contact vibrations, which are far from linear dynamics. Thus, to analyse machine tools vibrations, non-linear models of contact and non-linear dynamics should be applied. Hence, the contact vibrations and resonances should be studied under a wide range of excitation signals, while simplified linear models of contact rough surfaces do not allow the proper modelling of complex dynamical phenomena.

References

1. Awrejcewicz J., 1996, *Deterministic Vibrations of Discrete Systems*, WNT, Warszawa
2. Belhaq M., Fahsi A., 2009, Hysteresis suppression for primary and subharmonic 3:1 resonances using fast excitation, *Nonlinear Dynamics*, **57**, 1/2, 275-287
3. Bogusz W., Engel Z., Giergiel J., 1974, Oscillations and noise. Printed series of course lectures No. 347. University of Mining and Metallurgy, Kraków, Poland, *Wydawnictwa Geologiczne*, Warszawa, Poland
4. Chajkin S.E., Lisovskij L.N., Solomonović A.E., 1939, On the dry friction forces, *Doklady Akademii Nauk SSSR*, **24**, 134-138 [in Russian]
5. Chlebus E., Dybala B., 1999, Modelling and calculation of properties of sliding guide ways, *International Journal of Machine Tools and Manufacture*, **39**, 12, 1823-1839
6. Cunningham W.J., 1958, *Introduction to Nonlinear Analysis*, McGraw-Hill, New York
7. Dhupia J., Powalka B., Katz R., Ulsoy A.G., 2007, Dynamics of the arch-type reconfigurable machine tool, *International Journal of Machine Tools and Manufacture*, **47**, 2, 326-334
8. Fan K.C., Chen H.M., Kuo T.H., 2012, Prediction of machining accuracy degradation of machine tools, *Precision Engineering*, **36**, 2, 288-298
9. Fyrillas M.M., Szeri A.J., 1998, Control of ultra- and subharmonic resonances, *Journal of Nonlinear Science*, **8**, 2, 131-159
10. Grigorova S.R., Tolstoi D.M., 1966, On the resonance descending of friction force, *Doklady Akademii Nauk SSSR*, **167**, 562-563 [in Russian]
11. Grudziński K., Kostek R., 2007, An analysis of nonlinear normal contact microvibrations excited by a harmonic force, *Nonlinear Dynamics*, **50**, 4, 809-815

12. Gutowski P., 2003, Identyfikacja parametrów modeli dynamicznych układów nośnych obrabiarek, *Prace Naukowe Politechniki Szczecińskiej Wydział Mechaniczny*, **574** [in Polish]

13. Hess D.P., Soom A., 1991a, Normal vibrations and friction under harmonic loads: Part I – Hertzian contacts, Part II – Rough planar contacts, *ASME Journal of Tribology*, **113**, 1, 80-86

14. Hess D.P., Soom A., 1991b, Normal vibrations and friction under harmonic loads: Part II – Rough planar contact, *ASME Journal of Tribology*, **113**, 1, 87-92

15. Hunt K.H., Crossley F.R.E., 1975, Coefficient of restitution interpreted as damping in vibroimpact, *ASME Journal of Applied Mechanics*, **42**, 2, 440-445

16. Huo D., Cheng K., Wardle F., 2010, A holistic integrated dynamic design and modelling approach applied to the development of ultra-precision micro-milling machines, *International Journal of Machine Tools and Manufacture*, **50**, 4, 335-343

17. Kaminskaya V.V., Levina Z.M., Reshetov D.N., 1960, *Staninyi korpusnye detali metallorezhushchikh stankov*, Mashgiz Moscow [in Russian]

18. Kligerman Y., 2003, Multiple solutions in dynamic contact problems with friction, [In:] *Proceedings of STLE/ASME International Tribology Conference*, Ponte Vedra Beach, FL, 1-8

19. Kostek R., 2002, Modelling and analysis of the natural frequency of an elastic body resting on rough surface, *Zeszyty Naukowe Katedry Mechaniki Stosowanej, Politechnika Śląska*, **18**, 213-218 [in Polish]

20. Kostek R., 2004, Investigations of the normal contact microvibrations and their influences on the reduction of the friction forces in a dynamical system, Ph.D. Thesis, Szczecin University of Technology, Szczecin, Poland [in Polish]

21. Kostek R., 2013a, An analysis of the primary and the superharmonic contact resonances – Part 1, *Journal of Theoretical and Applied Mechanics*, **51**, 2, 475-486

22. Kostek R., 2013b, An analysis of the primary and the superharmonic contact resonances – Part 2, *Journal of Theoretical and Applied Mechanics*, **51**, 3, 687-696

23. Kostek R., 2013c, Direct numerical methods dedicated to second-order ordinary differential equations, *Applied Mathematics and Computation*, **219**, 19, 10082-10095

24. Levina Z.M., Reshetov D.N., 1971, *Contact Stiffness of Machines*, Mashinostroyenie, Moscow [in Russian]

25. Marchelek K., 1974, *Dynamika obrabiarek*, WNT Warszawa [in Polish]

26. Martins J.A.C., Oden J.T., Simoes F.M.F., 1990, A study of static and kinetic friction, *International Journal of Engineering Science*, **28**, 1, 29-94

27. Moradi H., Bakhtiari-Nejad F., Movahhedy M.R., Ahmadian M.T., 2010, Nonlinear behaviour of the regenerative chatter in turning process with a worn tool: Forced oscillation and stability analysis, *Mechanism and Machine Theory*, **45**, 8, 1050-1066

28. Nayak P. R., 1972, Contact vibrations, *Journal of Sound and Vibration*, **22**, 3, 297-322

29. Nayfeh A.H., 1983, The response of single degree of freedom systems with quadratic and cubic non-linearities to a subharmonic excitation, *Journal of Sound and Vibration*, **89**, 4, 457-470

30. Nayfeh A.H., Mook D.T., 1995, *Nonlinear Oscillations*, Wiley, New York

31. Neugebauer R., Denkena B., Wegener K., 2007, Mechatronic systems for machine tools, *CIRP Annals – Manufacturing Technology*, **56**, 2, 657-686

32. Parlitz U., Lauterborn W., 1985, Superstructure in the bifurcation set of the Duffing equation $\ddot{x} + d\dot{x} + x + x^3 = f\cos(\omega t)$, *Physics Letters A*, **107**, 8, 351-355

33. Perret-Liaudet J., 1998, Superharmonic resonance of order two on a sphere-plane contact, *Comptes Rendus de l'Acadmie des Sciences – Series IIB*, **326**, 12, 787-792

34. Perret-Liaudet J., Rigad E., 2007, Superharmonic resonance of order 2 for an impacting Hertzian contact oscillator: Theory and experiments, *ASME Journal of Computational and Nonlinear Dynamics*, **2**, 2, 190-196

35. Rigaud E., Perret-Liaudet J., 2003, Experiments and numerical results on non-linear vibrations of an impacting Hertzian contact: Part 1: harmonic excitation, *Journal of Sound and Vibration*, **265**, 2, 289-307

36. Shi X., Polycarpou A.A., 2005, Measurement and modelling of normal contact stiffness and contact damping at the meso scale, *ASME Journal of vibration and acoustics*, **127**, 1, 52-60

37. Skrodzewicz J., 2003, Influence of the lubricating agent on the properties of contact joints, *Journal of Theoretical and Applied Mechanics*, **41**, 1, 107-118

38. Skrodzewicz J., Gutowski P., 2000, Nonlinear mathematical models of weakly loaded contact joints, *Journal of Theoretical and Applied Mechanics*, **38**, 4, 781-785

39. Tang J., 2000, The MLP method for subharmonic and ultraharmonic resonance solutions of strongly nonlinear systems, *Applied Mathematics and Mechanics*, **21**, 10, 1153-1160

40. Thomas T. R., 1999, *Rough Surfaces*, Imperial College Press, UK

41. Thompson J.M.T., Stewart H.B., 2002, *Nonlinear Dynamics and Chaos*, Wiley, Chichester, UK

42. Tolstoi D.M., 1967, Significance of the normal degree of freedom and natural normal vibrations in contact friction, *Wear*, **10**, 3, 199-213

Manuscript received September 30, 2012; accepted for print November 26, 2012